

Abstract.—A commercially valuable trap fishery for spiny lobster (*Panulirus marginatus*) has existed in the Northwestern Hawaiian Islands since the late 1970s. Fisheries landings and research trapping show that spawning biomass and recruitment to the fishery collapsed in 1990 in the northern portion of the fishing ground and that there has been no recovery to the present, although recruitment remained strong at banks 670 km to the southeast. An advection-diffusion model is used to investigate larval transport dynamics between these two regions. The movement model is driven by geostrophic currents computed every 10 days from sea surface height obtained from TOPEX-POSEIDON satellite altimetry. The larval transport simulations indicate that even though larvae have a pelagic period of 12 months, banks differ substantially in the proportion of larvae they retain from resident spawners as well as the proportion of larvae they receive from other banks. In particular, recruitment to the northern portion of the fishing grounds is weak due to a very low local spawning biomass and a very limited contribution of larvae from the area of strong recruitment and high spawning biomass in the southeast. The results also suggest that satellite altimetry can provide useful information on physical dynamics for recruitment studies.

Application of TOPEX-POSEIDON satellite altimetry to simulate transport dynamics of larvae of spiny lobster, *Panulirus marginatus*, in the Northwestern Hawaiian Islands, 1993–1996

Jeffrey J. Polovina

Pierre Kleiber

Donald R. Kobayashi

Honolulu Laboratory, Southwest Fisheries Science Center

National Marine Fisheries Service, NOAA

2570 Dole Street, Honolulu, Hawaii 96822-2396

E-mail address (for J. J. Polovina): Jeffrey.Polovina@noaa.gov

The spiny lobster, *Panulirus marginatus*, is endemic to the Hawaiian Archipelago and Johnston Atoll. The species is found throughout the archipelago and is the target of a trap fishery in the northwestern portion of the archipelago known as the Northwestern Hawaiian Islands (NWHI). From the early 1980s to 1990, the majority of fishery catches came from two banks, Necker Island and Maro Reef, located 670 km northwest of Necker Island (Fig. 1). Catches during this period averaged about 60% from Maro Reef, 40% from Necker Island. However, in 1990 there was a dramatic collapse in recruitment of 3-year-old lobsters to the fishery at Maro Reef, and other banks north of Maro; this collapse has been attributed to climate-induced change in productivity that has impacted various other trophic levels, such as sea birds, monk seals, and reef fishes (Polovina et al., 1994). After the recruitment collapse, the fishery reduced the spawning biomass to very low levels at Maro and at other northern banks, and then fishing ceased in these areas. Even with the absence of fishing at Maro for at least six years, there is still no evidence of a recovery in recruitment as indicated from a time series of the

relative abundance of 3-year-olds obtained from a standardized research survey (Fig. 2). However, at Necker, 670 nmi to the southeast, the recruitment drop at the end of the 1980s was much less severe and recovery has occurred in recent years and has supported a fishery (Fig. 2). The striking differences in recruitment levels over the past seven years between the two banks raises the possibility that there is limited larval mixing between the two banks.

Current management for the lobster fishery is based on the hypothesis that recruitment to the NWHI banks comes from a well-mixed pool of larvae with contributions from the entire archipelago, and this pool of larvae oscillates seasonally along the archipelago, pushed northwest in the spring and summer with tradewind-driven Ekman transport and pushed back southeast in the fall and winter with westerly wind-driven Ekman transport (MacDonald, 1986). A genetic analysis during 1978–80 examined allozyme variation in spiny lobsters from seven banks covering a substantial spatial range of the Hawaiian Archipelago and found no evidence of genetic differentiation between banks (Shaklee and Samollow, 1984). However, a subsequent study in 1987, using a

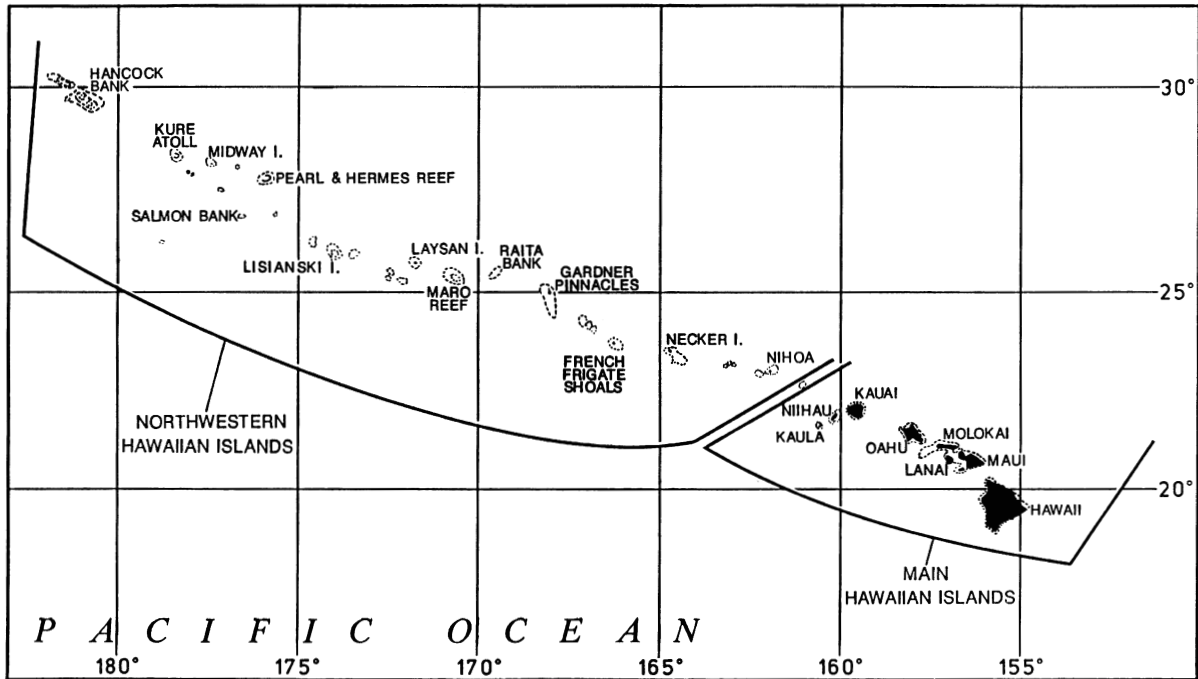


Figure 1
The Hawaiian Archipelago.

large sample size and comparing just Maro and Necker, found a statistically significant difference in allele frequency between Necker and Maro for one of the seven loci analyzed, raising the possibility that larval transport between the two banks may be limited (Seeb et. al., 1990).

The importance of Ekman transport in larval dynamics is not known, but larval sampling has found that a significant larval density exists well below the shallow Ekman layer and, in particular, that larvae appear to make diurnal movements from about 80–100 m in the day to 10–20 m at night (Polovina and Moffitt, 1995). Thus larval transport may be more influenced by transport of the mixed layer or geostrophic transport than by Ekman transport. The importance of geostrophic transport is also supported by correlations between sea-level height from tide gauges and spatial patterns in the subsequent fishery catches (Polovina and Mitchum, 1992, 1994). Indeed, the flat, leaf-like shape of spiny lobster larvae suggests they are adapted for passive horizontal transport assisted by vertical migration within the mixed layer (Lipcius and Cobb, 1994). The Hawaiian Archipelago lies near the center of the Sub-tropical Gyre; therefore the geostrophic transport

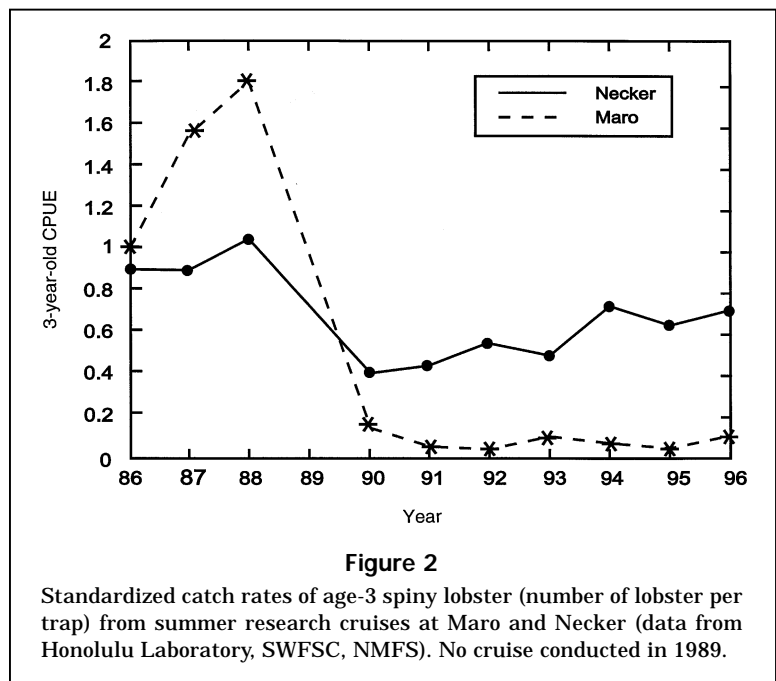


Figure 2
Standardized catch rates of age-3 spiny lobster (number of lobster per trap) from summer research cruises at Maro and Necker (data from Honolulu Laboratory, SWFSC, NMFS). No cruise conducted in 1989.

consists of weak flow from northwest to southeast along the archipelago, turning to the east at the southern end of the archipelago. Although the mean geostrophic transport is weak, geostrophic mesoscale features, particularly eddies, are prevalent and are likely to be significant for larval spatial dynamics.

Since late 1992, data have been collected by TOPEX-POSEIDON (T-P) satellite altimetry and are available in near-real time. The satellite covers the ocean over a 10-day period, providing a temporal resolution of 10 days; however, the spatial coverage is along narrow tracks; therefore interpolation between track is required for full spatial coverage. We used this altimetry data to estimate geostrophic current and ultimately to drive a simulation model of the transport of spiny lobster larvae released from selected banks in order to describe the spatial and seasonal dynamics of larval transport. In particular, in the NWHI, the spiny lobsters spawn in the summer, during May–August, and in the winter, during November and December, and the larvae are estimated to have a pelagic duration of 12 months (Polovina and Moffitt, 1995). We investigated aspects of the spatial and temporal dynamics of spiny lobster larval transport by simulating the movement of larvae from several representative banks from summer and winter spawning over the 12-month larval duration.

Methods

Topex altimetry data

The altimetry data used in this study were obtained from a 2-day Delayed Altimeter Data project of the Laboratory for Satellite Altimetry, National Environ-

mental Satellite, Data and Information Service (NESDIS), National Oceanic and Atmospheric Administration (NOAA), Department of Commerce. This project was a joint endeavor with the Naval Oceanographic Office (NOO) and the Jet Propulsion Laboratory (JPL). The altimetry data were first transmitted from the satellite to JPL, where the orbit position was finalized with the aid of GPS tracking data. NOO scientists performed an initial adjustment to the altimetry data using the JPL orbit information, then the data were forwarded to NOAA where a final orbit-related adjustment was made after the complete 10-day cycle of data was received. The data were aggregated into 1-degree latitude intervals along the satellite track (Fig. 3) and were expressed as a deviation from a 3-year (1993–95) mean altimetry. These data can be downloaded from an anonymous file transfer protocol (ftp) at

[falcon.grdl.noaa.gov in/pub/topex_real_time](ftp://falcon.grdl.noaa.gov/in/pub/topex_real_time)

or from an internet webpage at

http://ibis.grdl.noaa.gov/SAT/near_rt/topex_2day.html.

The data were ready for public dissemination approximately 2 days after each 10-day satellite cycle was completed. Altimetry data that were not aggregated but were continuous along track lines are avail-

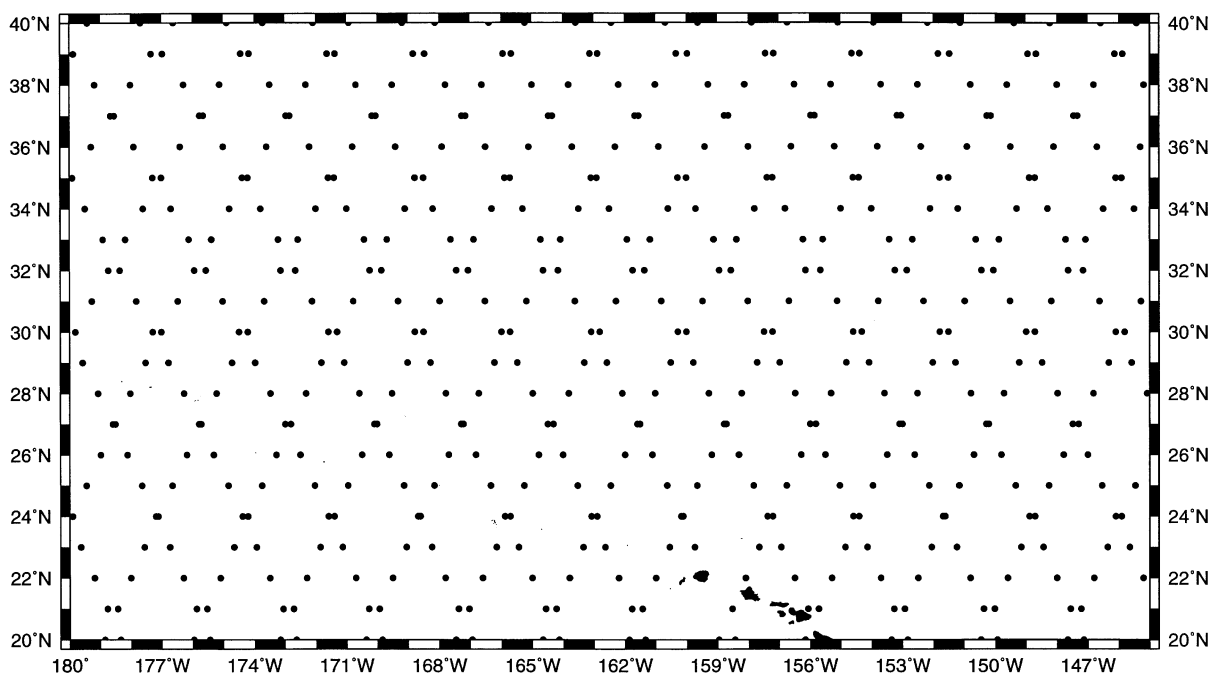


Figure 3
Spatial grid of near-real time TOPEX-POSEIDON data from a 10-day cycle.

able on CD-ROM from JPL. However, a considerable time lag may be associated with releases of these data.

After the data were downloaded, a unix shell script was used to process the individual cycle data. This script uses various subroutines of the Generic Mapping Tools (GMT) software package (the GMT software package is available from an anonymous ftp at [kiawe.soest.hawaii.edu](http://kiawe.soest.hawaii.edu/pub/gmt) in `/pub/gmt`). The GMT script first smoothed and then interpolated the data using a subroutine called “nearneighbor.” This subroutine placed the irregularly spaced track data onto a uniformly spaced latitude-longitude matrix, assigning values to each latitude-longitude location (node). Each node was assigned a weighted mean of all data points within a user-specified search radius (SR); i.e. a mean of all data within a geographic circle about each node. The weighting factor was a function of radial distance from the node such that $w(r) = 1/(1 + (3r/SR)^2)$, hence $w(r)$ ranged nonlinearly from 1 at the node ($r=0$) to 0.1 at SR units from the node ($r=SR$). When all orbital passes of the satellite cycle were complete, a SR value of 3 degrees could adequately interpolate regions between passes, independent of the relative date of the pass within the 10-day cycle, resulting in a complete grid file. For cycles with missing passes, the SR was able to be increased accordingly. The SR could also be specified as an absolute distance to ensure that the smoothing region was circular and not ovoid. After the deviation data were assembled on a grid, the script then added these data to another grid of equal dimensions containing the Levitus long-term mean dynamic height at 1000 m, which we assumed was representative of the mean dynamic topography for 1993–96. The Levitus data originated from the 1994 NODC World Ocean Atlas (CD-ROM data set), U.S. Department of Commerce, NOAA, National Environmental Satellite, Data, and Information Service (NESDIS). The grid file of absolute altimetry values (z) was then evaluated by the subroutine grid-gradient, which calculates the east-west and north-south gradients, dz/dx and dz/dy , where x and y and z are all in centimeters. These gradients were used for calculating the u and v components of the geostrophic current as follows:

$$u = -(g/f) \frac{dz}{dy} \quad (1)$$

and

$$v = (g/f) \frac{dz}{dx},$$

where $g = 980 \text{ cm per second}^2$;
 $f = 2 \Omega \sin \phi$;

$$\Omega = 7.29 \times 10^{-5} \text{ radians per second (earth angular rotational velocity); and}$$

$$\phi = \text{latitude.}$$

These u and v values represent estimates at the surface. They can also serve as estimates of geostrophic current over the top 100-m mixed layer if integrals over the mixed layer of the horizontal density gradients are negligible. For the region of interest in our study, given the weak horizontal density gradients, the error in using these surface estimates as mixed layer estimates, according to calculations with the Levitus density field, was less than 2 cm/s. This is negligible given the time and space scales we were considering.

The u and v values were then output to an ASCII file at 0.5-degree resolution. A separate file for each 10-day period ($n=169$ from Oct 92 to Jun 97) was constructed for the entire Topex-Poseidon data set. The GMT script optionally produced a contour map of dynamic height with an overlay of geostrophic current vectors for each cycle. The resultant maps showed eddy and meander features that were likely important in recruitment processes (Fig. 4).

Several authors have found excellent agreement between currents estimated from T-P data and ground-truthing. Comparisons between the current estimated from satellite-tracked drogued buoys and geostrophic current estimated from T-P data in the western Pacific resulted in correlations of 0.924 for zonal velocity (u) and 0.760 for meridional velocity (v) (Yu et al., 1995). Comparisons between current speed from an acoustic Doppler current profiler along T-P track lines in the Hawaiian Archipelago agreed with estimates from T-P to within a few cm/sec (Mitchum, 1996). Sea surface height from T-P and a large set of island tide gauges, including those in the Hawaiian Archipelago, yielded a correlation of 0.66 (Mitchum, 1994).

Movement model

Individual larvae were tracked for a series of time steps starting from a given location by iteratively applying advective displacements due to water flow with additional random displacements caused by diffusion. The position of each larva was updated at each time step as follows:

$$x_{t+\Delta t} = x_t + \left[u_{(x_t, y_t, t)} \Delta t + \varepsilon \sqrt{D \Delta t} \right] / \cos(y_t) \quad (2)$$

$$y_{t+\Delta t} = y_t + \left[v_{(x_t, y_t, t)} \Delta t + \varepsilon \sqrt{D \Delta t} \right],$$

where $t =$ time in days;

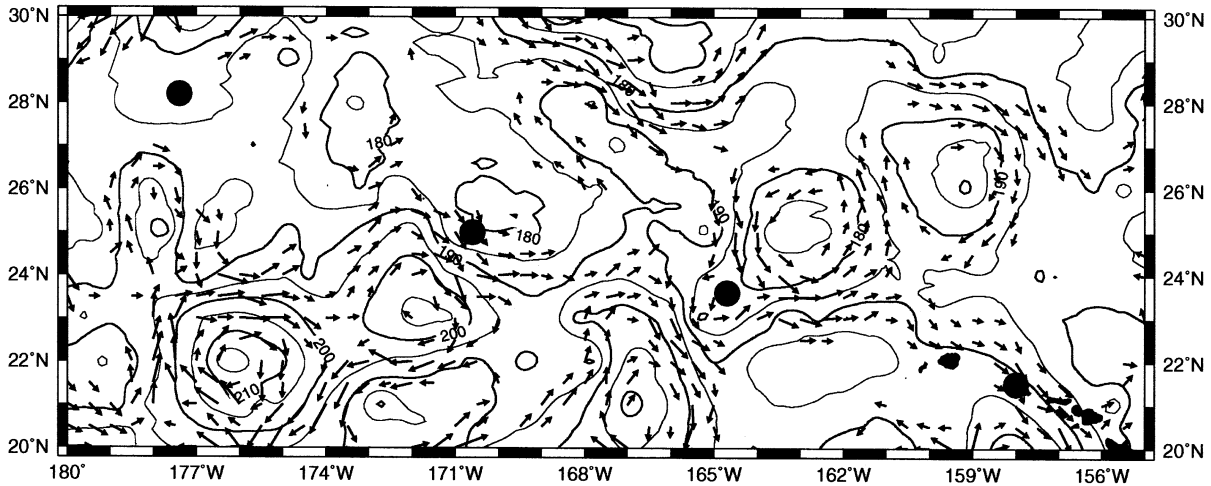


Figure 4

Sea surface height and geostrophic current estimated from a 10-day TOPEX/POSEIDON cycle, 16–26 August 1993. Only currents 8 cm/sec or larger are plotted with arrows. Solid circles from lower right (east) to upper left (west), denote Oahu, Necker, Maro, and Midway Islands, respectively.

- x and y = the larval position in degrees of longitude and latitude respectively;
- u and v = longitudinal and latitudinal components of velocity in degrees/day;
- ϵ = a normal (mean 0, standard deviation 1) random variate; and
- D = the eddy diffusion rate in units of degree²/day ($1 \text{ m}^2/\text{sec} = 7 \times 10^{-6} \text{ degree}^2/\text{day}$).

The first term in brackets in each equation is advective displacement and the second term, diffusional displacement. The cosine function in the longitudinal movement equation corrects for the fact that distance per degree of longitude decreases from the equator to the poles.

Values of u and v at particular locations and times were obtained by linear interpolation from the precalculated 0.5 degree by 10-day grid of u and v values computed from the T-P data. The time step was set to one day ($\Delta t=1$) with 365 iterations for one year of simulation. The 1-day time step was used to match the spatial resolution of the velocity field, but simulations showed that the choice of time step was robust up to about two weeks. Larvae dispersed in the model because a different diffusional displacement (a different ϵ) was chosen for each larva at each time step. Once larvae were even slightly separated, dispersal was further advanced because the larvae experienced different advective displacements as u and v varied spatially.

Simulations

Although lobsters presumably spawn on all banks in the Hawaiian Archipelago, for simplicity, the simu-

lations released larvae from only four banks: Midway and Oahu (chosen as representative of the northwestern and southeastern ends of the archipelago) and Necker and Maro (representative of the main fishing banks [Fig. 1]). Each simulation released 5000 larvae at the beginning of the month from each of the four banks for the four months of the summer spawning season and the two months of the winter spawning season from 1993 to 1995. The simulations tracked the positions of all released larvae for 365 days; no larval mortality was assumed. For example, Figure 5 shows the distribution of simulated larvae 180 and 365 days after release at Maro Reef in July 1995. The distribution showed patchiness caused by underlying oceanographic features and expanded spatially over time. This simulation was based on an eddy diffusion rate of $1000 \text{ m}^2/\text{sec}$, and the same simulation, but with the diffusion rate reduced to $100 \text{ m}^2/\text{sec}$, showed a striking increase in patchiness and the same general dispersal (Fig. 6). The eddy diffusion rate for the NWHI is not known, but a range from $100 \text{ m}^2/\text{sec}$ to $1000 \text{ m}^2/\text{sec}$ has been proposed for another large archipelago, the Great Barrier Reef (Gabric and Parslow, 1994). Because the level of diffusion rate impacts larval patchiness and because we had a measure of actual larvae patchiness from numerous larval tows throughout the archipelago (Polovina and Moffitt, 1995), we decided the appropriate level for eddy diffusion rate by comparing the frequency distribution of larvae sampled in actual larval tows with the frequency distribution of larvae from line transects and the simulated spatial patterns for different eddy diffusion-rate values. The frequency distribution from transects with an eddy

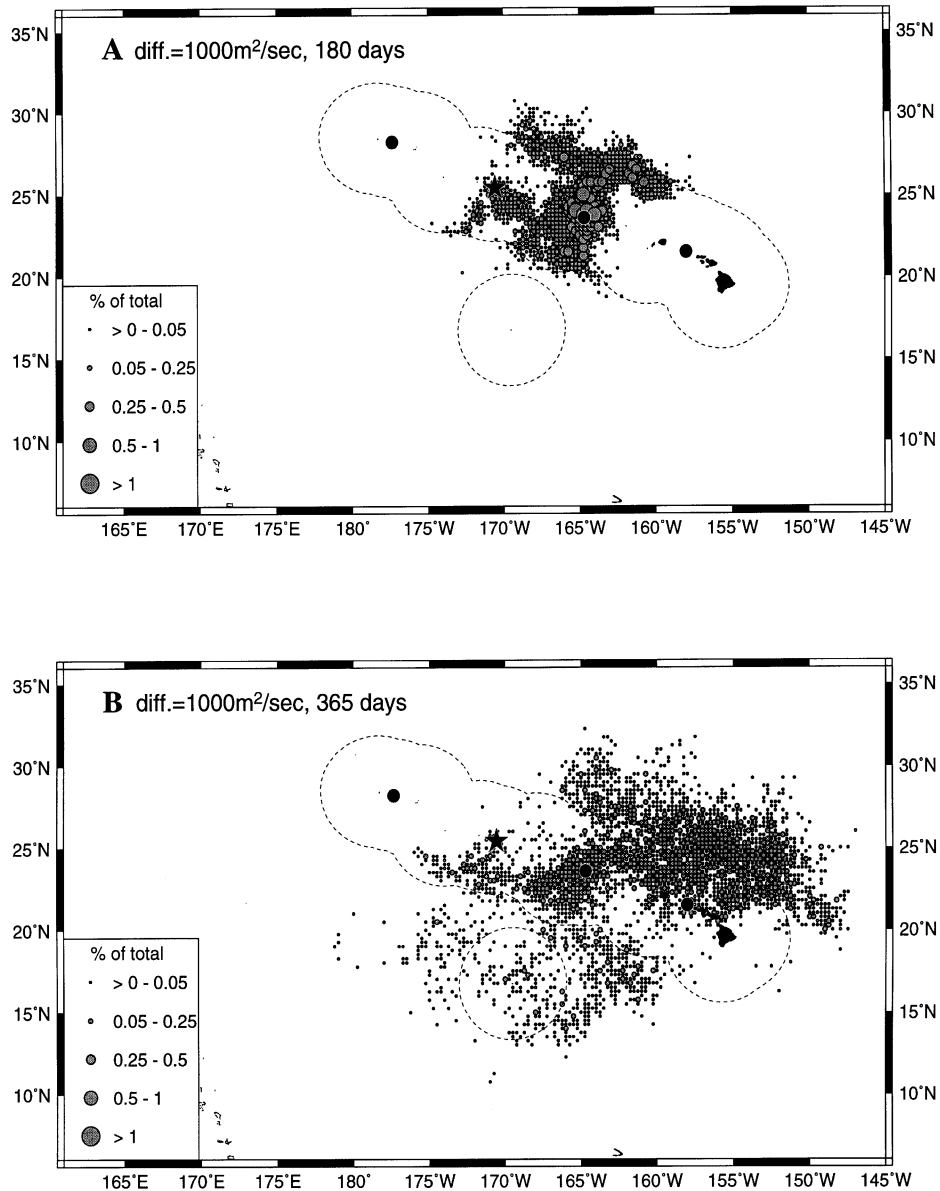


Figure 5

Simulated spatial distribution of 5000 larvae (A) 180 and (B) 365 days after release on 1 July 1995 at Maro with an eddy diffusion rate of 1000 m²/sec. Solid circles denote Oahu, Necker, and Midway Islands, and the star marks Maro Island.

diffusion rate of 1000 m²/sec had a lognormal distribution but underrepresented the heavy tails of the actual larval-tow frequency distribution. The frequency distribution from transects with an eddy diffusion rate of 100 m²/sec had extremely heavy tails, in fact bimodal distribution. Either very few larvae were encountered or many larvae were encountered, resulting in a distribution that had too many large clumps compared with the observed distribution. However, an eddy diffusion rate of 500 m²/sec produced a larval frequency distribution that closely

matched the distribution from the larval tows, and this value was used in all subsequent simulations.

At the end of their larval period, spiny lobster larvae metamorphose into pueruli that, at least for other spiny lobster species, are capable of directed horizontal swimming over 40–60 km (Pearce and Phillips, 1994). For *P. marginatus*, it is not known how close a larva needs to be to a bank at the end of its larval period to recruit to that bank. The 200-m isobath around the islands and banks of the archipelago is generally circular and marks the points at

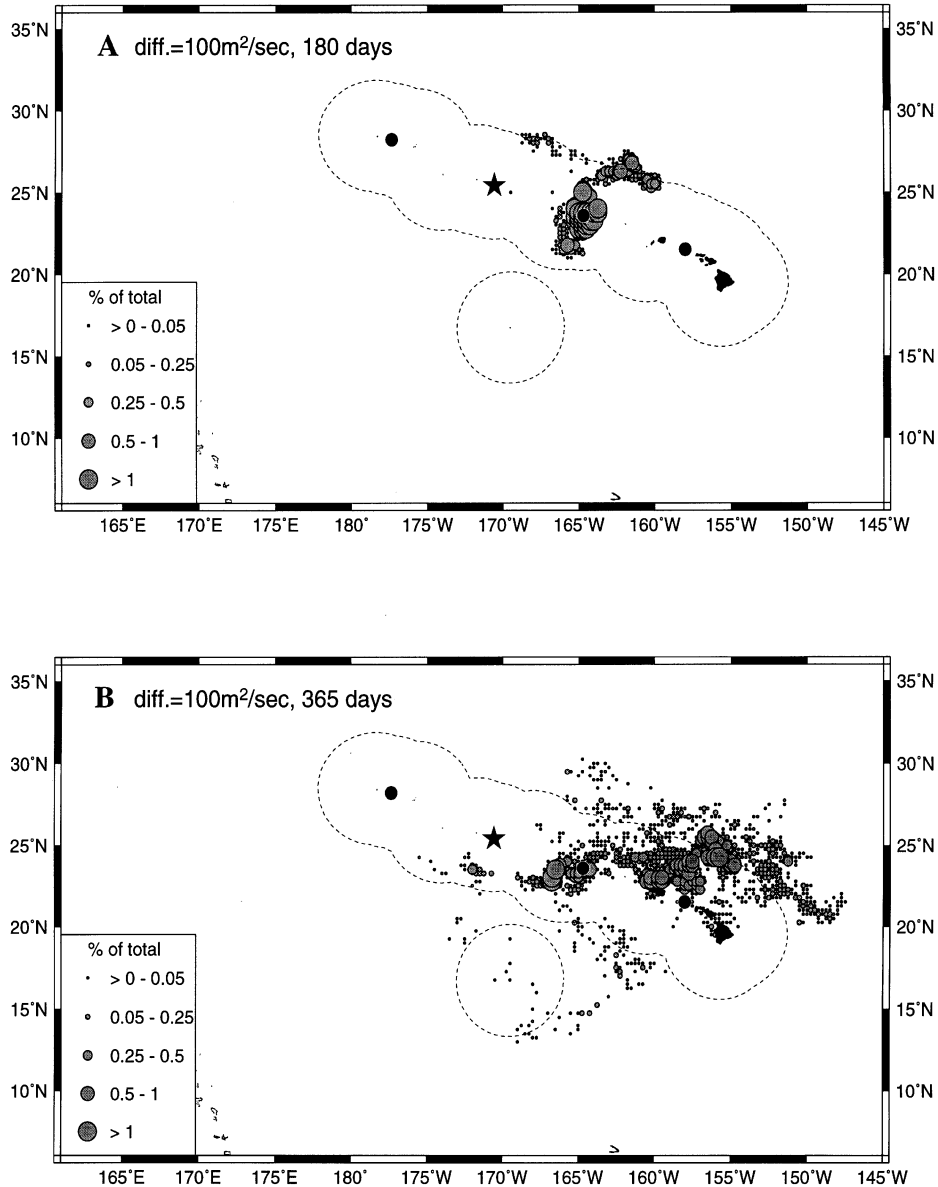


Figure 6

Simulated spatial distribution of 5000 larvae (**A**) 180 and (**B**) 365 days after release on 1 July 1995 at Maro with an eddy diffusion rate of $100 \text{ m}^2/\text{sec}$. Solid circles denote Oahu, Necker, and Midway Islands, and the star marks Maro Island.

which the topography drops steeply to midocean depths. For Necker, Maro, and Oahu, the radius of the 200-m isobath is about 70 km. Oceanographic features resulting from interactions with topography that larvae might detect will certainly extend some distance beyond the 200-m isobath, perhaps a distance equal to the radius of the bank. Thus, as an index of larval recruitment to a bank, we assumed that larvae that were within 140 km of a bank 365 days after release would recruit to that bank. The choice of 140 km was somewhat arbitrary but because we used the index as a relative and not abso-

lute index, the results were not particularly sensitive to this distance.

Results

Simulations were performed to describe the larval spatial dynamics from 5000 larvae released from all four banks for the 4-month summer spawning season (May–August) and the 2-month winter spawning season (November and December). The results indicated that there are spatially distinct patterns that generally persist

between years and spawning seasons and that were seen, for example, in the distribution of 1-year-old larvae in July 1995 (Fig. 7). Larvae released from Midway were advected eastward, larvae from Maro were advected east and south, larvae from Necker were advected east and south, and larvae from Oahu were advected primarily southwest (Fig. 7). A fairly persistent meander at about 26°N concentrated larvae zonally, whereas persistent westward flow at the southern end of the archipelago advected Oahu larvae westward (Fig. 7). At the center of the archipelago, specifically at Maro and Necker, a substantial portion of larvae remained close to the bank where they were spawned, even after 12 months, whereas at the ends of the archipelago, at Midway and Oahu, advection was high (Fig. 7). Further, although Necker receives abundant larvae spawned at Maro, relatively few larvae from Necker reached Maro (Fig. 7). The results, averaged over three years, showed that the percentage of larvae released at a bank and that were within 140 km of that bank 365 days later varied considerably by bank (Table 1). Differences in this percentage between winter and summer spawning seasons were not generally large but the interannual range of this percentage often varied more than threefold (Table 1). Averaged over all three years and over the two spawning seasons, the percent of larvae within 140 km of a bank 365 days after being released at that bank was 5.5%, 9.6%, 16.7%, and 16.6% for Midway, Maro, Necker, and Oahu, respectively (Table 1).

From the three years of simulations, no radical changes from the bank-specific larval distribution patterns shown in Figure 7 were seen, only spatial extensions or contractions. For example, the distribution of larvae 365 days after spawning at Necker had a northeast and southwest orientation, and larvae spawned in 1993 at Necker Island were advected east and southwest to a greater extent than larvae in 1994 or 1995 (Fig. 8).

Table 1
Mean percentage of larvae that were within 140 km of their bank of origin 365 days after release, 1993–96.

Release season	Bank	Mean percent (interannual range)
Summer	Midway	3.1 (1.8–4.7)
	Maro	10.4 (3.9–20.4)
	Necker	15.7 (9.5–20.3)
	Oahu	11.7 (8.4–15.9)
Winter	Midway	7.9 (3.7–15.0)
	Maro	8.8 (4.9–13.8)
	Necker	18.0 (8.9–29.4)
	Oahu	21.4 (12.1–33.3)

To examine the exchange of larvae between banks, the recruitment index was calculated on the basis of the bank at which the larvae originated, for both summer and winter spawning seasons, with 5000 larvae released from each bank (Table 2). The results were similar for both spawning seasons. Recruitment to Midway came almost entirely from larvae spawned at Midway. Recruitment to Maro was based largely on larvae from Maro and Midway; only 10–21% of the recruits at Maro came from Necker and Oahu. Necker had the broadest geographic source of recruits, receiving substantial larvae from all four banks. Oahu’s recruits come from Maro, Necker, and Oahu (Table 2).

Discussion

The altimetry data from T-P provide a new tool to investigate recruitment questions. However, this approach has several limitations. First, because the geoid is not known, an estimate of mean dynamic topography (Levitus) was added to the T-P sea surface height anomalies. Although the accuracy of the

Table 2
Mean percentage of 12-month larvae within 140 km of each bank by bank of origin, 1993–96.

Release season	Destination bank	Bank of origin			
		Midway	Maro	Necker	Oahu
Summer	Midway	100	0	0	0
	Maro	59	31	9	1
	Necker	5	47	32	16
	Oahu	0	28	41	31
Winter	Midway	91	7	2	0
	Maro	49	30	18	3
	Necker	10	29	37	24
	Oahu	0	19	31	50

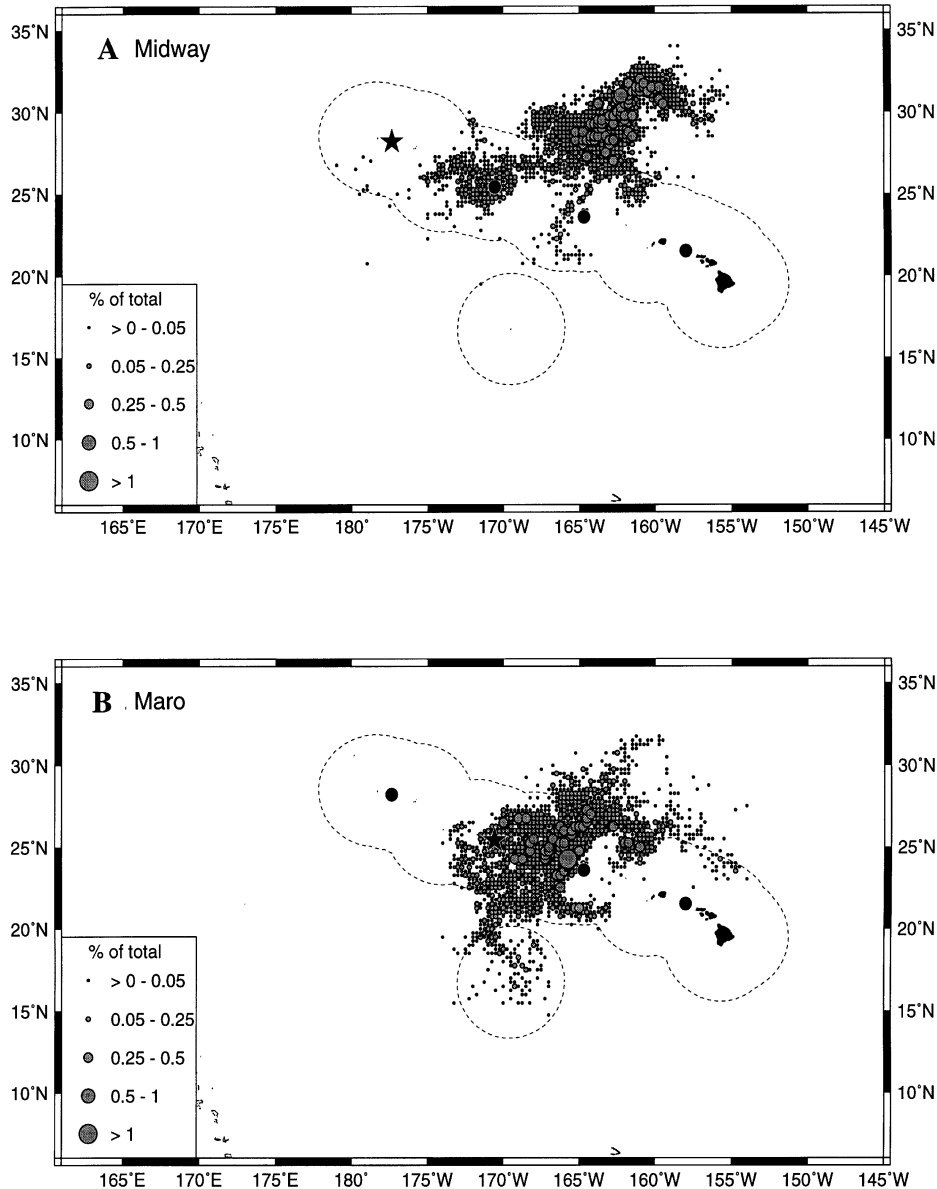


Figure 7

Simulated spatial distribution of 5000 larvae 365 days after release on 1 July 1994 at (A) Midway, (B) Maro, (C) Necker, and (D) Oahu, with an eddy diffusion rate of $500 \text{ m}^2/\text{sec}$. The star denotes the bank from which larvae were released. Solid circles mark the other three banks.

Levitus mean varied depending on the spatial and temporal distribution of the underlying data, it was likely that there were biases that may have had an impact on the accuracy of the estimates of absolute geostrophic current. A second limitation is that the spacing between data tracks, especially in mid- and low-latitude regions, may have been too broad to completely resolve many important finescale and mesoscale physical features. Further, this tool is appropriate only in situations where geostrophic transport is the most significant source of larval transport, situ-

ations, for example, where larvae are below the shallow Ekman layer.

In our application, this approach leads to a new hypothesis on the spatial dynamics of lobster larval recruitment in the Hawaiian Archipelago. From the simulations, we found that position of a spawning bank within the archipelago influences both the number of larvae spawned at a bank that will recruit to that bank as well as the recruitment that a bank will receive from other banks. Specifically, the results indicated that larvae are transported down the ridge from the north-

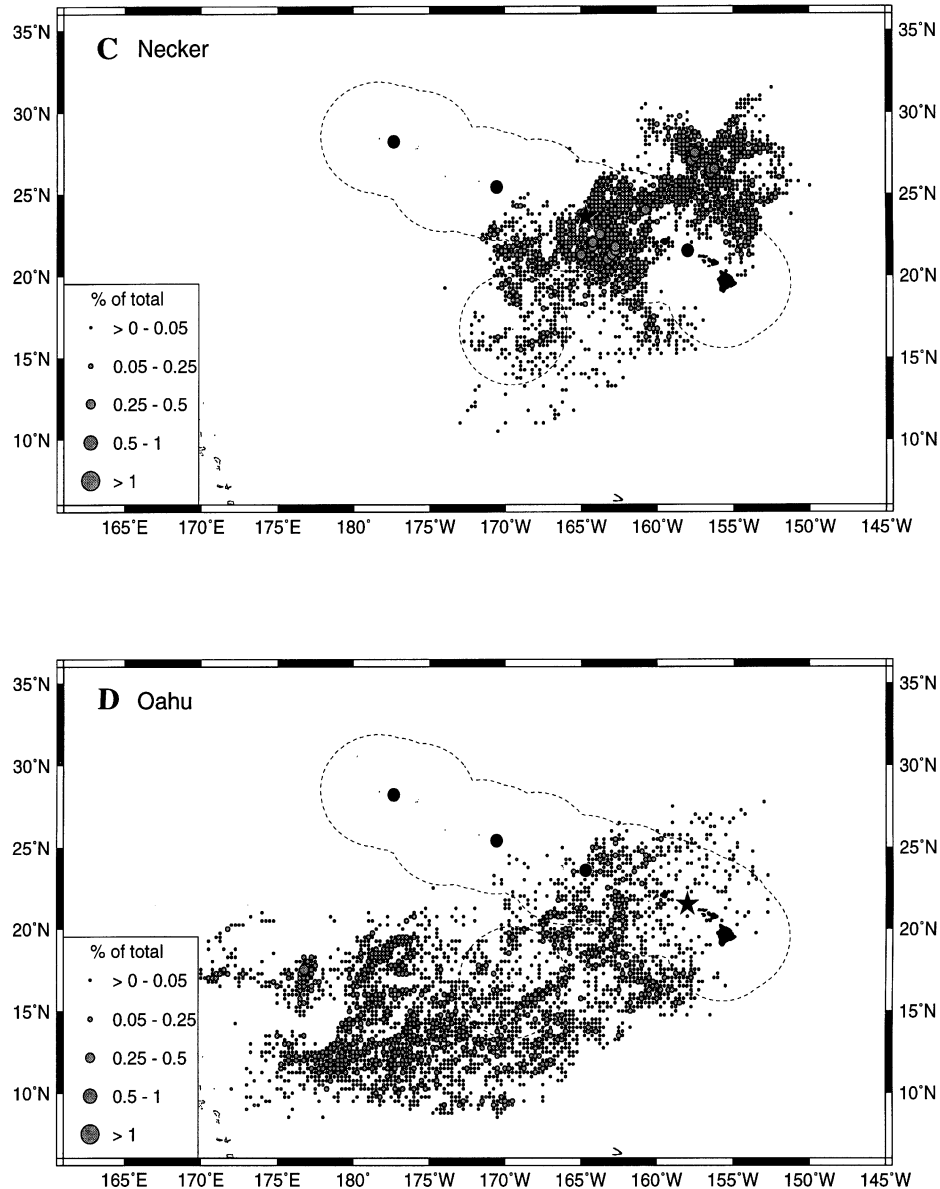


Figure 7 (continued)

west to the southeast to Necker and then southwest. Necker's persistent spiny lobster population and fishery appear to be the result of its location where it both receives larvae from banks to the northwest and southeast and also has a high retention of its own larvae. Only 670 km to the northwest, Maro's retention rate was only about one-half that of Necker, and although it contributed larvae to Necker, it did not receive any substantial contribution of larvae from Necker. This finding explains why recruitment at Maro remained depressed once the spawning biomass at Maro and other banks to the northwest were depleted, even though there was a substantial spawning biomass at Necker. However, it raises questions. Why were Maro and other northern banks so productive during the

1980s? Was the transport regime in the 1980s different, so that Maro and northern banks lost fewer larvae to the southeast and perhaps even received considerable larvae from Necker? Alternatively, because the fishery began only in the late 1970s, was recruitment always so weak at Maro and at other northern banks that the collapse at the end of the 1980s represented simply a response to overfishing an unexploited population? Although we cannot answer these questions, the results suggest that if the transport regime observed during 1993–96 persists, increased recruitment to Maro and other banks to the northwest may require an increase in the spawning population at Maro and other northern banks. Research on a similar species of spiny lobster, *P. argus*, in the Bahamas found physical trans-

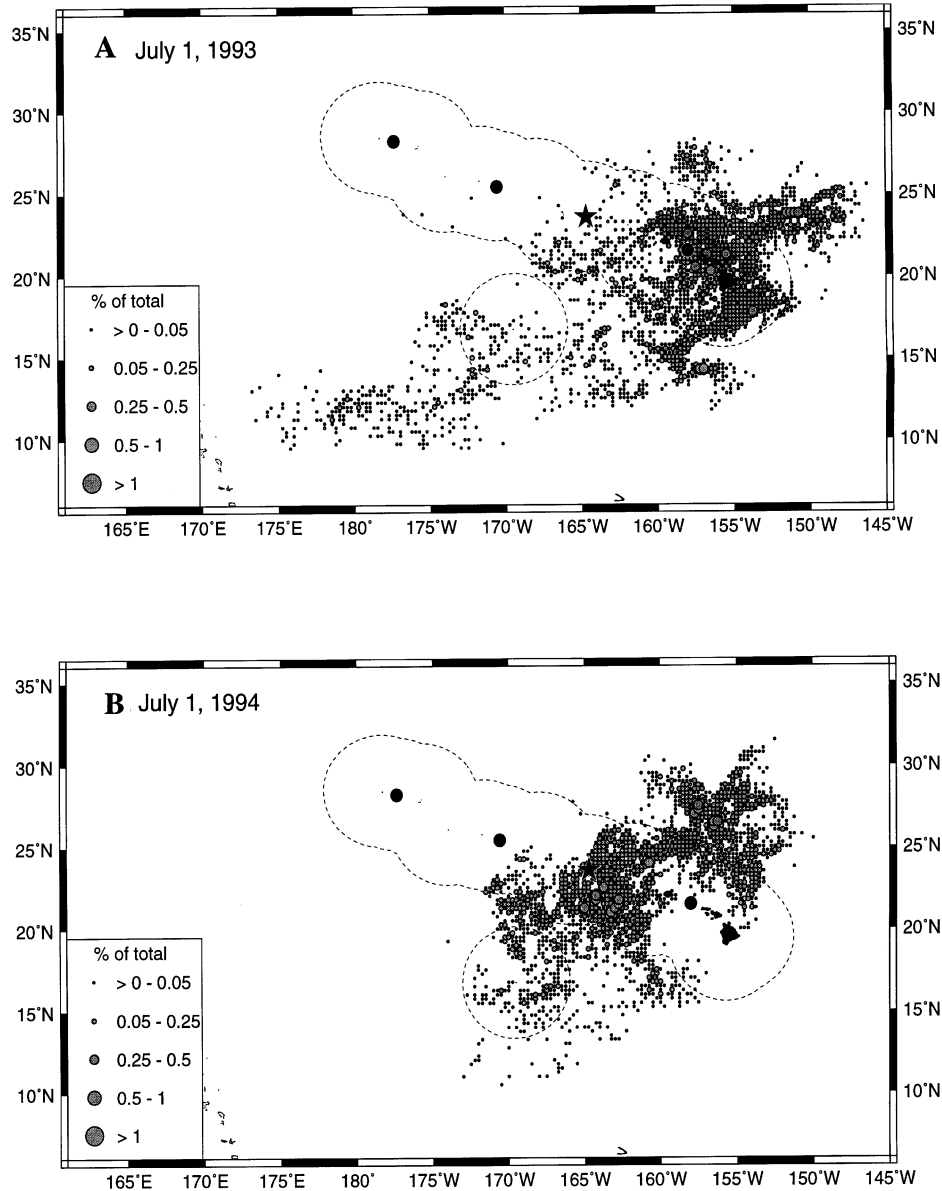


Figure 8

Simulated spatial distribution of 5000 larvae 365 days after release at Necker on (A) 1 July 1993, (B) 1 July 1994, and (C) 1 July 1995, with an eddy diffusion rate of 500 m^2/sec . Solid circles denote Oahu, Maro, and Midway Islands, and the star marks Necker Island.

port important to the spatial distribution of larvae (Lipcius et al., in press).

However, it is important to remember that larval abundance is necessary but not always sufficient for good recruitment and that other factors, such as habitat and predators, may also be important. Further, work to improve the input parameters and to validate these simulation results is certainly needed. For example, the results are certainly sensitive to the larval depth distribution as a function of larval age. Because these simulations produce near-real time spatial distribu-

tions, larval surveys could be designed to sample larvae in areas where the simulations show high and low larval densities in order to evaluate the model results. The model results can also be evaluated by comparing bank-specific recruitment index time series against estimated recruitment to the fishery three years later. Further, genetic studies based on DNA analyses may be more sensitive than the earlier electrophoretic studies in testing the apparent lack of mixing between regions of the archipelago suggested by these simulations. Given the hypothesis that transport was generally from

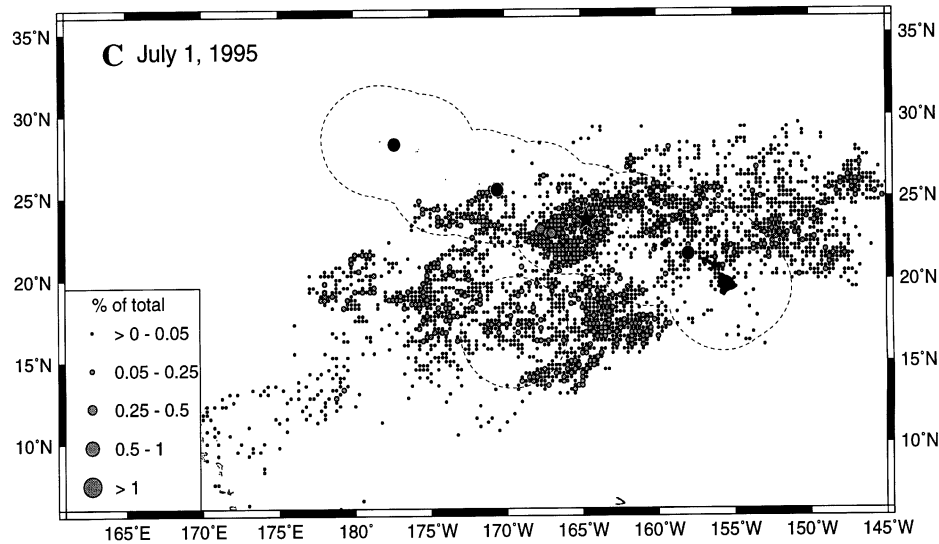


Figure 8 (continued)

Midway to Necker, this results in a testable hypothesis that genetic variance should be greater at Necker than at Midway.

Acknowledgments

Dawn Lambeth, a NSF Research Experience for Undergraduates recipient, provided a great deal of assistance in programming and running the simulation model. The senior author gratefully acknowledges the contributions from many valuable discussions on satellite altimetry and physical oceanography with Professor Gary Mitchum, University of South Florida. This work was partially funded by Cooperative Agreement Number NA37RJ0199 from NOAA.

Literature cited

- Gabric, A. J., and J. Parslow.**
1994. Factors affecting larval dispersion in the central Great Barrier Reef. In P. W. Sammarco and M. L. Herson (eds.), The bio-physics of marine larval dispersal, p. 149–158. Coastal and Estuarine Studies (45), AGU, Washington, D.C.
- Lipcius, R. N., and J. S. Cobb.**
1994. Ecology and fishery biology of spiny lobsters. In B. F. Phillips et al. (eds.), Spiny lobster management, p. 1–30. Fishing News Books, Oxford, England.
- Lipcius, R. N., W. T. Stockhausen, D. B. Eggleston, L. S. Marshall Jr., and B. Hickey.**
In press. Hydrodynamic decoupling of recruitment, habitat quality, and adult abundance in the Caribbean spiny lobster: source-sink dynamics. Mar. Freshwater Res.
- MacDonald, C. D.**
1986. Recruitment of the puerulus of the spiny lobster, *Panulirus marginatus*, in Hawaii. Can. J. Fish. Aquat. Sci. 43:2111–2125.
- Mitchum, G. T.**
1994. Comparison of the topex sea surface heights and tide gauge sea level. J. Geophys. Res. 99:24,541–25,553.
1996. On using satellite altimetric heights to provide a spatial context for the Hawaii Ocean time-series measurements. Deep-Sea Res. 43(2–3):257–280.
- Pearce, A. F., and B. F. Phillips.**
1994. Oceanic processes, puerulus settlement and recruitment of the western rock lobster *Panulirus cygnus*. In P. W. Sammarco and M. L. Herson (eds.), The bio-physics of marine larval dispersal, p. 279–306. Coastal and Estuarine Studies (45), AGU, Washington, D.C.
- Polovina, J. J., and G. T. Mitchum.**
1992. Variability in spiny lobster, *Panulirus marginatus*, recruitment and sea level in the Northwestern Hawaiian Islands. Fish. Bull. 90:483–49.
1994. Spiny lobster recruitment and sea level: results of a 1990 forecast. Fish. Bull. 92(1):203–205.
- Polovina, J. J., G. T. Mitchum, N. E. Graham, M. P. Craig, E. E. Demartini, and E. N. Flint.**
1994. Physical and biological consequences of a climate event in the central North Pacific. Fish. Oceanogr. 3(1):15–21.
- Polovina, J. J., and R. B. Moffitt.**
1995. Spatial and temporal distribution of the phyllosoma of the spiny lobster, *Panulirus marginatus*, in the Northwestern Hawaiian Islands. Bull. Mar. Sci. 56(2): 406–417.
- Seeb, L. W., J. E. Seeb, and J. J. Polovina.**
1990. Genetic variation in highly exploited spiny lobster, *Panulirus marginatus*, populations from the Hawaiian Archipelago. Fish. Bull. 88:713–718.
- Shaklee, J. B., and P. B. Samollow.**
1984. Genetic variation and population structure in a spiny lobster, *Panulirus marginatus*, in the Hawaiian archipelago. Fish. Bull. 82:693–702.
- Yu, Y., W. J. Emery, and R. R. Leben.**
1995. Satellite altimeter derived geostrophic currents in the western tropical Pacific during 1992–1993 and their validation with drifting buoy trajectories. J. Geophys. Res. 100 (C12):25069–25085.